



Universiteit
Leiden
The Netherlands

Interaction of oxygen and carbon monoxide with Pt(111) at intermediate pressure and temperature : revisiting the fruit fly of surface science

Bashlakov, D.

Citation

Bashlakov, D. (2014, October 14). *Interaction of oxygen and carbon monoxide with Pt(111) at intermediate pressure and temperature : revisiting the fruit fly of surface science*. Retrieved from <https://hdl.handle.net/1887/29023>

Version: Corrected Publisher's Version

License: [Licence agreement concerning inclusion of doctoral thesis in the Institutional Repository of the University of Leiden](#)

Downloaded from: <https://hdl.handle.net/1887/29023>

Note: To cite this publication please use the final published version (if applicable).

Cover Page



Universiteit Leiden

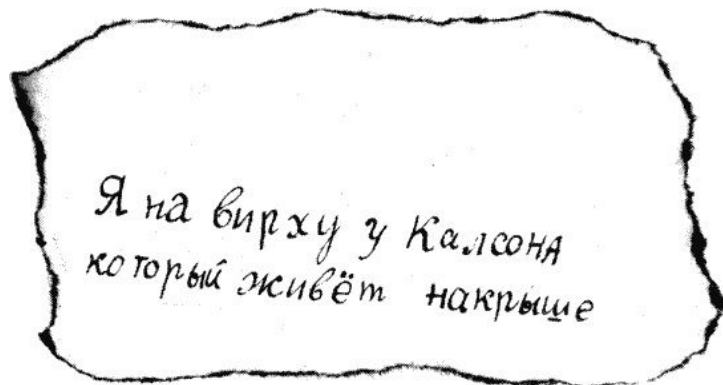


The handle <http://hdl.handle.net/1887/29023> holds various files of this Leiden University dissertation

Author: Bashlakov, Dmytro

Title: Interaction of oxygen and carbon monoxide with Pt(111) at intermediate pressure and temperature : revisiting the fruit fly of surface science

Issue Date: 2014-10-14



Chapter 1

Introduction and literature overview

1.1. Introduction

Evolution and industrialization of human society is tightly connected to the use of metals. The first countries in the modern meaning of this word (distinct borders, defined policy and society organization) appear in the Bronze Age, when humans learned how to smelt and handle copper. Since then, metals began to be used not only for “primitive work” but also for specific “smart” applications. Besides being good construction materials due to their strength and plasticity, their unique electronic properties allow them to be used in functional devices. It is hard to imagine the functioning of the Large Hadron Collider without the niobium-titanium alloy used in the superconducting magnets or the development of modern computers without hard disc drives employing the giant magneto-resistance effect for information storage.

The application of metals as catalysts revolutionized the emerging chemical industry as well. Steam reforming is one of many examples of current industrial scale production of chemicals. Here, nickel is used for the production of hydrogen from fossil fuels and water. This reaction is the main source of hydrogen for ammonia production in the Haber-Bosch process [1]. In this nitrogen fixation reaction, NH_3 is synthesized from nitrogen and hydrogen with the help of iron as a catalyst. As the initial component for artificial fertilizers, ammonia now “feeds” the continually growing population of the planet. A major advantage of using metals in industrial catalysis is that they are present as a solid during the reaction. It simplifies technological processes for the separation of products, which are typically present in the gas or liquid phase.

The demand for renewable energy sources as a basis for developing the post-industrial society delivers new challenges for commercial use of metals. Hydrogen is nowadays considered an alternative for fossil fuels. In the “Hydrogen Economy”, the target is an infrastructure where hydrogen is used as the energy carrier. Even though the process seems economically viable, at present steam reforming of methane can only be a temporary solution for the production of hydrogen as it consumes fossil fuels [2]. Electrolysis of water run on “green” electricity (wind, sunlight, hydropower, etc.) can be a permanent solution for this task.

Platinum is part of the puzzle for developing a closed materials cycle-renewable energy system. Its application in fuel cells already provides an alternative for combustion engines for transportation. In dye-sensitized solar cells platinum is used as a cathode. These cells are more attractive for household applications than semiconductor analogs due to the number of advantages such as smaller weight, lower production costs, and ability to work at low light intensity [3]. The real challenge for fundamental science now is to answer the question: “Why are some materials so unique?” Fully understanding the physics and chemistry may eliminate the need for expensive catalytic materials such as platinum by substitution with cheaper analogs providing similar performance.

This thesis uses the surface science approach to address questions regarding the interaction of oxygen with platinum and its subsequent reaction with carbon monoxide. A Pt(111) single crystal surface is used as a model for the catalyst. Chapter 1 provides an overview of the literature on the subject. The description of employed experimental techniques and their backgrounds are presented in Chapter 2. Chapter 3 discusses the adsorption of oxygen on Pt(111) at various temperatures and its role in the oxidation of carbon monoxide. Chapter 4 gives an atomic scale insight into the reaction between adsorbed oxygen and carbon monoxide for different ratios of oxygen and carbon monoxide pressures. In Chapter 5, the reaction between CO and oxygen on Pt(111) was used to register noise in tunneling current due to diffusion and recombination of molecules on the catalytically active surface, to draw conclusions on the most likely rate-limiting step in the process.

1.2. Catalysis

As stated previously, catalysis plays a major role in the industrial production of chemicals. The additional component needed to increase the reaction rate is called “catalyst”. A catalyst is involved temporarily in the chemical path of the reaction but does not appear as a final product. The principal scheme of a catalytic reaction can be described with the potential energy diagram (Figure 1.1) where the initial and the final states of the system are presented for the reactants **A** and **B** and the reaction product **P_{AB}**, respectively. In a non-catalyzed reaction, the final state is reached by overcoming a potential energy barrier with activation energy **E_a**. The particular task of the catalyst is to provide an alternative path for the

reaction with smaller activation energy E_a . In such case, a single reaction event proceeds via binding both or one of the reactants **A** and **B** to the catalyst first. Subsequently, reaction between reactants occurs with an activation energy smaller than for the non-catalyzed reaction. Finally, the formed product P_{AB} detaches from the catalyst so that the latter returns to its initial state and the next binding-reaction-detaching cycle can proceed.

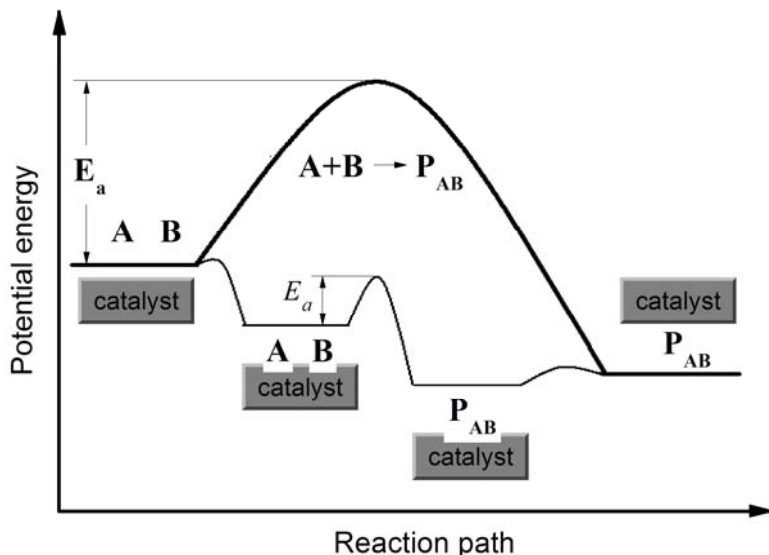


Figure 1.1. Potential energy diagram for a non-catalyzed and catalyzed reaction (reproduced from [4]).

There is a continuous search for better catalysts in order to optimize existing chemical processes as well as to introduce new ones. The performance of the catalyst is characterized by its activity, selectivity and stability. The meaning of these properties can also be explained by using the simple picture of the potential energy diagram:

- i. *Activity* of the catalyst describes how much product can be produced in the catalytic reaction over a period of time. The amount of product is determined by the activation energy E_a in such a way that the time needed for a single reaction reduces with the lowering of E_a . As a consequence, a catalyst with lower activation energy will convert more species **A** and **B** into P_{AB} over a certain period of time and will show higher activity (reaction rate) than a catalyst with higher activation energy under otherwise identical conditions.

- ii. If the desired product of reaction is the chemical P_{AB} , formation of different species (P_{BB} , P_{AA} , P_{ABA} , etc.) leads to an ineffective use of the feedstock. If the catalyst serves to reduce the activation energy only for the desired product (P_{AB}) while the reaction path for other species remains unchanged or becomes more difficult, the catalyst *selectively* accelerates the reaction for useful product.
- iii. *Stability* indicates how long a catalyst can serve before losing its catalytic properties. Theoretically, the $A + B \xrightarrow{\text{catalyst}} P_{AB}$ reaction cycle can be repeated indefinitely, however, the side products (like P_{BB} , P_{AA} , P_{ABA} , etc.) can also bind to the catalyst. If this chemical bond is strong, all active sites will be blocked after some time by the side products and the catalyst will lose its activity. A stable catalytic performance can also be influenced by the morphological changes of a catalyst.

The field of catalysis can be roughly divided in two parts. In homogeneous catalysis the reactant and catalyst are present in the same phase. In heterogeneous catalysis the catalyst and reactants are in different phases. To a large extent, industrial catalysis relies on heterogeneous catalysis where metal surfaces serve to bind reactants from the gaseous or liquid phase. A concept first introduced by Irving Langmuir [5] states that the surface serves as a two-dimensional lattice for molecular adsorption. The adsorbed molecules or atoms can diffuse across the surface approaching each other for reaction or desorb back into the gas/liquid. The rate of reaction strongly depends on the adsorption energy (i.e. the energy levels of adsorbed **A** and **B** in Figure 1.1) of the molecules to the surface and is described by the Sabatier principle [1]: The interaction of the adsorbants and the surface should be just right to obtain maximum reaction rate (activity). If the molecules are bound too weakly, they can leave the surface before reaction occurs. For very high adsorption energies, molecules will accumulate on the surface and block the active sites for adsorption of the new reactants, thus causing deactivation of the catalyst.

1.3. Surface science approach

Time dependent product analysis for an industrial catalyst is typically performed with techniques such as chromatography or mass spectrometry. This approach is useful in collecting information about the overall catalyst activity, selectivity and stability, while varying the macroscopic parameters

of reaction (temperature, pressure, reactants composition, etc.). The whole system, however, remains a “black box” for understanding fundamental steps of reaction. This is mostly due to the complex structure of the catalyst. Catalytically active nanoparticles are not uniform and are generally deposited onto an inactive support that often has little or no long-range structure. It is difficult to separate the contributions to the overall reaction rate from different crystal facets of the nanoparticles. The *surface science approach* studies catalytic reactions on well defined single crystal surfaces (Figure 1.2). In case of reactants present in the gas phase, the single crystal is cleaned and stored under UHV conditions ($\sim 10^{-10}$ mbar) prior to its exposure to the reactants.

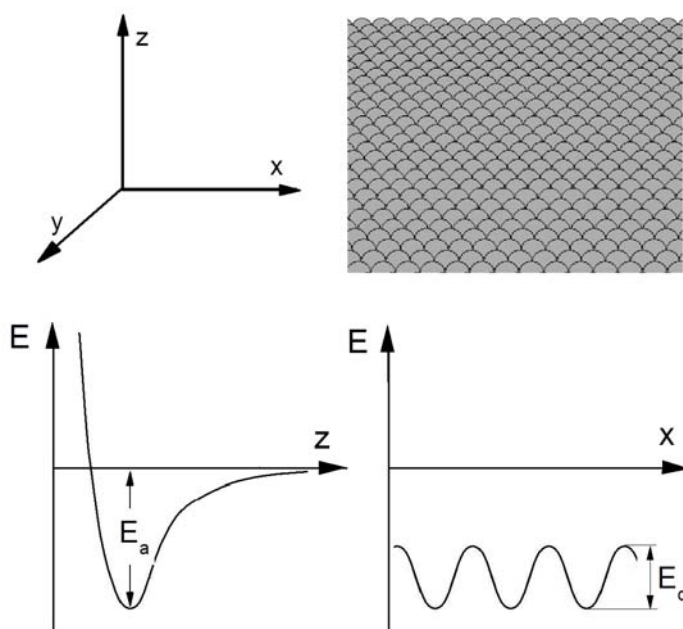


Figure 1.2. Potential energy diagram in direction perpendicular to the surface (bottom left) and along the surface (bottom right) for an adsorbate on a single crystal surface (top right), reproduced from [7].

The interaction between adsorbates and the surface can be illustrated with the potential energy diagram [6] shown on Figure 1.2. The minimum energy of the system is defined by the equilibrium state in which repulsive and attraction forces compensate each other. The repulsion force acts between the ionic cores of adsorbates and surface atoms. The attraction involves either van der Waals interactions (physisorption) or formation of a

chemical bond between molecules/atoms and surface (chemisorption). The position of the minimum in the energy diagram defines the distance of a molecule from the surface in the adsorbed state, while the decrease in the potential energy relative to the state for infinite distance z between adsorbate and the surface can be seen as the adsorption energy E_a of this molecule.

The binding energy of an adsorbate depends on its position on the surface [8]. The surface can be seen as a matrix of adsorption sites with largest adsorption energies (lowest potential energies) separated by a potential energy barrier (E_d). To move across the surface, an adsorbate has to jump over this potential barrier. Figure 1.2 represents a potential energy surface for the diffusion of an adsorbate along the x direction. The average time τ an adsorbate stays in one adsorption site can be estimated as [7]:

$$\tau \sim \exp\left(-\frac{E_d}{kT}\right),$$

so, that at low temperatures ($kT \ll E_d$), an adsorbate will stay in the adsorption site almost indefinitely. For $kT \geq E_d$ the residence time of adsorbate is limited and it can move across the surface if the nearest adsorption sites are not all occupied. If an adsorbed particle is surrounded by others, it will stay in the same adsorption site, unless it has energy higher than E_a to return into the gas phase (desorb) or react with a neighbor. When all adsorption sites are occupied, the surface has reached the saturation coverage $\theta = n_a/n_s$, where n_a and n_s are the maximum density of adsorbed particles and the density of atoms on the surface of the catalyst, respectively.

The previous description is valid if there is no possibility for recombinative desorption or other forms of reaction. Otherwise, when $E_a > kT \geq E_d$ adsorbed molecules/atoms can approach and react with each other by forming a new molecule. The latter will leave the surface if the condition $E_a^{\text{new molecule}} < kT$ is valid.

As mentioned above, the research subjects of this thesis are the adsorption of oxygen and the reaction between oxygen and carbon monoxide on the Pt(111) surface. Detailed knowledge about adsorption sites of O and CO and the mechanism of chemisorption is essential to understand the reaction path of O and CO reacting to CO_2 . A brief summary of the state-of-the-art of these three topics is given in the next three sections.

1.3.1. Oxygen interaction with Pt(111)

The interaction of molecular oxygen with platinum can be illustrated with the energy diagram of Figure 1.3a [6, 9]. In the final state of adsorption O_2 dissociates into two atoms by going through the intermediate state of chemisorbed O_2 . Indirectly, this path was observed first in TPD experiments for a cold Pt(111) surface exposed to O_2 [10, 11]. A subsequent linear increase of the sample temperature showed two desorption peaks for oxygen. The first desorption peak at 160 K was assigned to molecularly chemisorbed oxygen. A second broad peak with a maximum at ~ 750 K was assigned to recombinative desorption of atomic oxygen. Using electron energy loss spectroscopy (EELS) it was confirmed that two different types of oxygen are present on Pt(111) at temperatures above 160 K [12-14]. Insight into the dissociation mechanism was delivered later by STM experiments. These showed that O_2 adsorbs on bridge sites of platinum prior to dissociation and that oxygen atoms occupy three-fold hollow fcc sites after dissociation [15-17].

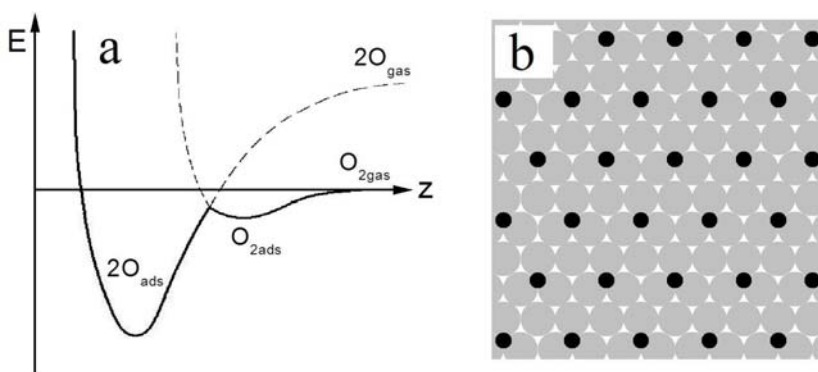


Figure 1.3. a) Energy diagram for dissociative adsorption of diatomic molecule (O_2). b) O -p(2x2)-Pt(111) surface structure with 0.25 ML coverage for the layer of atomic oxygen (black circles) dissociatively adsorbed onto the (111) platinum crystal plane (grey circles).

Continuous exposure of a Pt(111) surface to molecular oxygen at room temperature leads to the formation of a layer of atomic oxygen ordered into a p(2x2) structure [18, 19] as shown on Figure 1.3b. This layer is characterized by (2x2) diffraction patterns in low energy electron diffraction (LEED) [9, 20]. It is interesting to note that (2x2) patterns become visible long before the oxygen layer reaches saturation [9]. This observation is in

agreement with STM measurements [15] showing that oxygen atoms prefer to organize into $p(2 \times 2)$ islands indicating “an indirect attractive O-O interaction mediated through the electronic system of the substrate” [7].

Above room temperature, the mobility of platinum atoms starts to play a role in the interaction of platinum with oxygen [21, 22]. STM measurements showed significant restructuring (roughening) of Pt(110) and Pt(111) surfaces in an oxygen atmosphere of 1 bar at temperatures above 400 K [23, 24]. XRD studies reveal the formation of α -PtO₂ on both crystallographic surfaces at identical conditions [25, 26]. This oxide structure on Pt(111) was found to be stable for O₂ pressures down to 1 mbar [26] indicating that not only temperature but also oxygen pressure is important for the oxide formation. Although most studies for the O₂-Pt(111) system performed under high vacuum conditions did not focus on oxygen adsorption at temperatures above 300 K, some reported that at enhanced temperatures the amount of oxygen adsorbed on the Pt(111) surface is three to five times higher than expected from the O- $p(2 \times 2)$ layer [27-29]. Since platinum is a primary catalyst for oxidation reactions [1], an understanding of the alteration of catalytic properties of Pt(111) by high levels of surface oxidation is required [30, 31].

1.3.2. Carbon monoxide interaction with Pt(111)

Carbon monoxide chemisorbs on platinum as a diatomic molecule without dissociation [32] via formation of a chemical bond between carbon and platinum atoms [33]. The energy of this bond is rather low compared to the adsorption energy for atomic oxygen [34, 35]. Carbon monoxide desorbs from the Pt(111) surface at temperatures between 320-350 K, as derived from temperature programmed desorption (TPD) experiments [36-38]. EELS [38, 39] and infrared spectroscopy measurements [40, 41] reveal two types of adsorption sites: on-top of platinum atoms and on bridge sites between two platinum atoms. The difference between the CO adsorption energy for on-top and bridge sites is small [34, 42]. This causes high mobility of carbon monoxide on the platinum surface [34, 37]. The latter was noticed first in LEED experiments [32, 36]: the diffraction patterns from an unsaturated CO- $(\sqrt{3} \times \sqrt{3})R30^\circ$ -Pt(111) layer (Fig.1.4a) with 1/3 ML coverage became visible only after the sample was cooled sufficiently (150-170 K) [43]).

The saturation coverage of the CO-Pt(111) layer varies continuously with the CO pressure to which the surface is exposed [44]. A maximum

coverage of ~ 0.7 ML can be reached, depending on the adsorption conditions [36]. At high vacuum conditions (10^{-8} - 10^{-7} mbar) and room temperature, the equilibrium saturation coverage is 0.5 ML. The CO layer is ordered into a commensurate $c(4 \times 2)$ structure. This was initially concluded from LEED data [33] and later confirmed by scanning tunneling microscopy (STM) measurements [45]. In this structure, equal numbers of CO molecules adsorb on two high symmetry sites (on-top and bridge) as illustrated in Figure 1.4b. A coverage of CO molecules above 0.5 ML can be obtained under the high vacuum conditions by cooling the platinum surface below 170 K in a CO atmosphere [36, 38, 41] or by increasing the CO pressure above 10^{-6} mbar at room temperature [46]. Such treatment leads to restructuring of the $c(4 \times 2)$ layer into an incommensurate layer in which CO molecules are compressed closer to one other [47, 48] and the repulsive CO-CO interaction forces them to move from the high symmetry adsorption sites [47-49], as shown in Figure 1.4c.

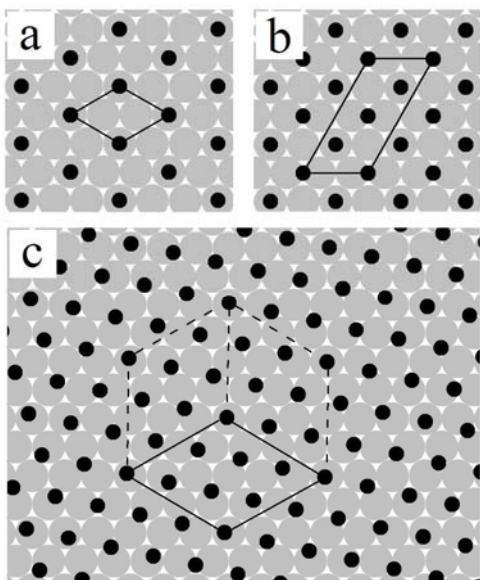
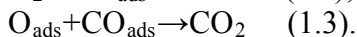


Figure 1.4. Platinum surface (grey circles) with carbon monoxide (black circles) adsorbed into: a) $(\sqrt{3} \times \sqrt{3})R30^\circ$ structure with $1/3$ ML coverage; b) $c(4 \times 2)$ structure with 0.5 ML coverage; c) incommensurate structure with CO coverage ≈ 0.56 ML.

1.3.3. CO oxidation on Pt(111)

The reaction of CO oxidation on platinum follows the Langmuir-Hinshelwood mechanism [50, 51], which states that both reactants are

adsorbed on the surface when the reaction occurs. The reaction steps can be described with following three equations:



Reaction step (1.2) is sensitive to the presence of CO on the surface in the way that increasing the CO coverage inhibits oxygen dissociation [52]. On the other hand, the oxygen-covered Pt(111) surface is open for CO adsorption [53, 54]. Therefore, in coadsorption/titration experiments oxygen is the first component to be adsorbed on the surface [50, 53-58]. Gland and Kollin [55] were the first to demonstrate that reaction step (1.3) is thermally activated. The formation of CO_2 happens at temperatures above 250 K. The activation energy for this reaction step was found to be different for a high oxygen coverage ($E_a \approx 0.5$ eV) compared to a low coverage of oxygen and CO ($E_a \geq 1$ eV) [50, 54-58]. Using DFT calculations Alavi et al. [59] obtained a potential barrier of 1eV for the recombination reaction between CO and the oxygen atom adsorbed in the configuration (I) shown in Figure 1.5.

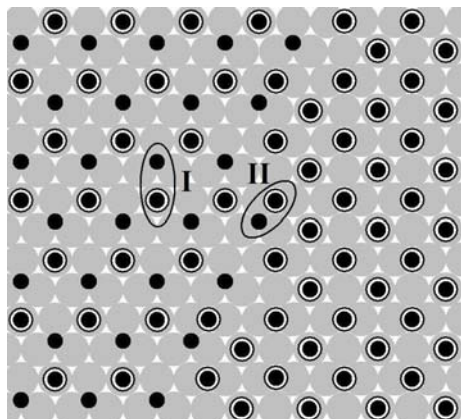


Figure 1.5. $p(2 \times 2)$ oxygen layer coadsorbed with CO (left part) in contact with $c(4 \times 2)$ layer of CO (right part) The oxygen atoms and CO molecules are shown by small black circles and white and black circles, respectively.

For a CO molecule placed at the bridge site closer to an oxygen atom (configuration II on Figure 1.5) the activation energy for reaction reduces to ≈ 0.5 eV. This suggests that in configuration (II) the activation time ($\tau \sim \exp(E_a/kT)$) for reaction step (1.3) is shorter than in configuration (I). STM titration experiments [58] confirmed that at the border between CO-O $p(2 \times 2)$ and CO-covered parts of the surface the reaction rate for O-CO recombination is higher than inside the CO-O $p(2 \times 2)$ islands. The results presented in the Chapter 4 of this thesis support this observation.

This brief overview shows that the general mechanism for the CO oxidation is well understood: two species pre-adsorbed on specific adsorption sites come together and associate. However, several aspects require more attention to form a complete atomistic picture, such as how the formation of the platinum surface oxide at elevated temperature [30, 31] impacts on CO oxidation and how the CO poisoning [53-58] ceases the steady state oxidation reaction.

Chapter 3 deals with the first question. The experiment, which combines Temperature Programmed Reaction Spectroscopy (TPRS), Low Energy Electron Diffraction (LEED) and Scanning Tunneling Microscopy (STM) measurements, demonstrates that the Pt(111) surface can dissociatively adsorb more oxygen than 0.25 ML. This happens when the surface is exposed to oxygen at high vacuum conditions and elevated temperatures (400-600 K). Part of the oxygen migrates into the subsurface region. Interestingly, subsurface oxygen shows a much lower reactivity toward the oxidation of co-adsorbed CO, and moreover it does not influence the oxidation properties of the surface-bound oxygen.

In Chapter 4 oxidation of CO is studied at room temperature with STM and LEED for different ratios of oxygen and CO pressures in the gas phase. It will be shown there that the difference in the adsorption mechanisms of O₂ and CO, leads to a different dynamics of CO poisoning of the Pt(111) surface. For ratios close to the CO poisoning regime, the surface reaction causes the formation of a complex surface structure consisting of separated islands of ordered oxygen atoms and disordered regions containing carbon monoxide. With excess CO in the gas mixture, the surface becomes covered by a CO layer which blocks O₂ dissociation. With excess O₂, the surface is covered by a p(2x2) oxygen layer, which remains active for CO→CO₂ conversion.

The attempt to measure the noise signature in the tunneling current during the surface reaction is described in Chapter 5. Based on the idea that recombination and diffusion of adsorbed species should cause changes in the local density of states on the surface, it was assumed that a higher noise level will be detected for the platinum surface brought in contact with gaseous mixture of CO and O₂ than for the platinum surface in vacuum. Indeed, an enhanced noise level compared to bare surface was observed experimentally for a Pt(111) surface in contact with O₂ and with a mixture of CO and O₂, suggesting that the mobility of O on the surface is responsible for the enhanced noise levels and may therefore be a slow step in the overall reaction rate.

References:

- [1] B. K. Hodnett, F. J. J. G. Janssen, J. W. Niemantsverdriet, V. Ponec, R. A. van Santen, and J. A. R. van Veen, *Catalysis: An Integrated Approach*, Elsevier Science, Amsterdam, 2000.
- [2] J. N. Armor, *Applied Catalysis A: General* 176 (1999) 159.
- [3] M. Gratzel, *Nature* 414 (2001) 338.
- [4] I. Chorkendorff and J. W. Niemantsverdriet, *Concept of modern catalysis and kinetics*, Wiley-VSH, Weinheim, 2003.
- [5] I. Langmuir, *Journal of the American Chemical Society* 40 (1918) 1361.
- [6] J. E. Lennard-Jones, *Transactions of the Faraday Society* 28 (1932) 333.
- [7] G. Ertl, *Reactions at solid surfaces*, Wiley, Berlin, 2009.
- [8] K. W. Kolasinski, *Surface Science: Foundation of Catalysis and Nanoscience*, Wiley, West Chester, 2008.
- [9] H. P. Bonzel and R. Ku, *Surface Science* 40 (1973) 85.
- [10] J. L. Gland, *Surface Science* 93 (1980) 487.
- [11] P. R. Norton, *Surface Science* 47 (1975) 98.
- [12] N. R. Avery, *Chemical Physics Letters* 96 (1983) 371.
- [13] P. Nolan, *The Journal of Chemical Physics* 111 (1999) 3696.
- [14] H. Steininger, S. Lehwald, and H. Ibach, *Surface Science* 123 (1982) 1.
- [15] B. C. Stipe, M. A. Rezaei, and W. Ho, *The Journal of Chemical Physics* 107 (1997) 6443.
- [16] J. Wintterlin, R. Schuster, and G. Ertl, *Physical Review Letters* 77 (1996) 123.
- [17] T. Zambelli, J. V. Barth, J. Wintterlin, and G. Ertl, *Nature* 390 (1997) 495.
- [18] K. Mortensen, C. Klink, F. Jensen, F. Besenbacher, and I. Stensgaard, *Surface Science* 220 (1989) L701.
- [19] P. R. Norton, J. A. Davies, and T. E. Jackman, *Surface Science* 122 (1982) L593.
- [20] J. Yoshinobu and M. Kawai, *The Journal of Chemical Physics* 103 (1995) 3220.
- [21] A. K. Galwey, P. Gray, J. F. Griffiths, and S. M. Hasko, *Nature* 313 (1985) 668.
- [22] C. Ellinger, A. Stierle, I. K. Robinson, A. Nefedov, and H. Dosch, *Journal of Physics-Condensed Matter* 20 (2008) 5.
- [23] B. L. M. Hendriksen and J. W. M. Frenken, *Physical Review Letters* 89 (2002) 046101.
- [24] S. C. Bobaru, Ph.D., Leiden University, The Netherlands, Leiden, 2006, p. 129.
- [25] M. D. Ackermann, T. M. Pedersen, B. L. M. Hendriksen, O. Robach, S. C. Bobaru, I. Popa, C. Quiros, H. Kim, B. Hammer, S. Ferrer, and J. W. M. Frenken, *Physical Review Letters* 95 (2005) 255505.

- [26] M. D. Ackermann, Ph.D., Leiden University, The Netherland, Leiden, 2007, p. 192.
- [27] D. Neuhaus, F. Joo, and B. Feuerbacher, *Physical Review Letters* 58 (1987) 694.
- [28] G. N. Derry and P. N. Ross, *Surface Science* 140 (1984) 165.
- [29] G. N. Derry and P. N. Ross, *Journal of Chemical Physics* 82 (1985) 2772.
- [30] W. X. Li and B. Hammer, *Chemical Physics Letters* 409 (2005) 1.
- [31] F. Gao, S. M. McClure, Y. Cai, K. K. Gath, Y. Wang, M. S. Chen, Q. L. Guo, and D. W. Goodman, *Surface Science* 603 (2009) 65.
- [32] H. Hopster and H. Ibach, *Surface Science* 77 (1978) 109.
- [33] D. F. Ogletree, M. A. Van Hove, and G. A. Somorjai, *Surface Science* 173 (1986) 351.
- [34] M. Lynch and P. Hu, *Surface Science* 458 (2000) 1.
- [35] Y. Y. Yeo, L. Vattuone, and D. A. King, *The Journal of Chemical Physics* 106 (1997) 392.
- [36] G. Ertl, M. Neumann, and K. M. Streit, *Surface Science* 64 (1977) 393.
- [37] C. T. Campbell, G. Ertl, H. Kuipers, and J. Segner, *Surface Science* 107 (1981) 207.
- [38] H. Steininger, S. Lehwald, and H. Ibach, *Surface Science* 123 (1982) 264.
- [39] H. Froitzheim, H. Hopster, H. Ibach, and S. Lehwald, *Applied Physics A: Materials Science & Processing* 13 (1977) 147.
- [40] H. Krebs and H. Lüth, *Applied Physics A: Materials Science & Processing* 14 (1977) 337.
- [41] B. N. J. Persson, M. Tushaus, and A. M. Bradshaw, *The Journal of Chemical Physics* 92 (1990) 5034.
- [42] E. Schweizer, B. N. J. Persson, M. Tüshaus, D. Hoge, and A. M. Bradshaw, *Surface Science* 213 (1989) 49.
- [43] J. S. McEwen, S. H. Payne, H. J. Kreuzer, M. Kinne, R. Denecke, and H. P. Steinruck, *Surface Science* 545 (2003) 47.
- [44] R. T. Vang, E. Laegsgaard, and F. Besenbacher, *Physical Chemistry Chemical Physics* 9 (2007) 3460.
- [45] M. O. Pedersen, M.-L. Bocquet, P. Sautet, E. Legsgaard, I. Stensgaard, and F. Besenbacher, *Chemical Physics Letters* 299 (1999) 403.
- [46] S. R. Longwitz, J. Schnadt, E. K. Vestergaard, R. T. Vang, I. Stensgaard, H. Brune, and F. Besenbacher, *The Journal of Physical Chemistry B* 108 (2004) 14497.
- [47] E. Kruse Vestergaard, P. Thostrup, T. An, E. Lægsgaard, I. Stensgaard, B. Hammer, and F. Besenbacher, *Physical Review Letters* 88 (2002) 259601.
- [48] M. Montano, K. Bratlie, M. Salmeron, and G. A. Somorjai, *Journal of the American Chemical Society* 128 (2006) 13229.
- [49] M. Tüshaus, W. Berndt, H. Conrad, A. M. Bradshaw, and B. Persson, *Applied Physics A: Materials Science & Processing* 51 (1990) 91.

- [50] C. T. Campbell, G. Ertl, H. Kuipers, and J. Segner, *The Journal of Chemical Physics* 73 (1980) 5862.
- [51] G. Ertl, *Surface Science* 299–300 (1994) 742.
- [52] M. Ehsasi, M. Matloch, O. Frank, J. H. Block, K. Christmann, F. S. Rys, and W. Hirschwald, *The Journal of Chemical Physics* 91 (1989) 4949.
- [53] J. L. Gland and E. B. Kollin, *Surface Science* 151 (1985) 260.
- [54] M. Kinne, T. Fuhrmann, J. F. Zhu, C. M. Whelan, R. Denecke, and H. P. Steinruck, *The Journal of Chemical Physics* 120 (2004) 7113.
- [55] J. L. Gland and E. B. Kollin, *The Journal of Chemical Physics* 78 (1983) 963.
- [56] I. Nakai, H. Kondoh, K. Amemiya, M. Nagasaka, T. Shimada, R. Yokota, A. Nambu, and T. Ohta, *The Journal of Chemical Physics* 122 (2005) 134709.
- [57] F. Zaera, J. Liu, and M. Xu, *The Journal of Chemical Physics* 106 (1997) 4204.
- [58] J. Wintterlin, S. Volkening, T. V. W. Janssens, T. Zambelli, and G. Ertl, *Science* 278 (1997) 1931.
- [59] A. Alavi, P. Hu, T. Deutsch, P. L. Silvestrelli, and J. r. Hutter, *Physical Review Letters* 80 (1998) 3650.

